

X-rays from Interacting and Merging Galaxies

K.J. Fricke and P. Papaderos

Universitäts-Sternwarte Göttingen, Geismarlandstraße 11, 37083 Göttingen, Germany

Abstract. We have used ROSAT PSPC and HRI to study the properties of the soft X-ray emission in a sample of colliding starburst galaxies. Together with data from other spectral ranges (optical, radio and FIR) we investigate the emergence of soft X-ray emission during progressive stages of interaction and merging.

1. Introduction

Interactions and merging of galaxies must be considered major drivers of galaxy evolution (morphology, spectral evolution, gas-dynamics, high-energy processes, AGN formation). A merger sequence for the formation of elliptical galaxies from interacting spirals was first proposed by Toomre (1977) based on numerical simulations. Inclusion of gas dynamics and star formation using Tree-SPH codes is now state of the art (cf. Mihos & Hernquist 1996) and allows a variety of predictions for the induced star formation and dynamical phenomena to be compared with observations. In Sect. 2 one of these systems, NGC 6240, is discussed in detail with respect to spatial structure, X-ray emission, optical colors, FIR-, and H α emission. Then we discuss the X-ray properties and X-ray evolution of a sample representing interacting and merging systems along the merger sequence and we look for systematic changes of the luminosities L_X , L_B , L_{FIR} , and the contribution of extended X-ray emission along that sequence.

2. NGC 6240

This system is in the stage of violent merging from the evidence of its extreme FIR luminosity (Soifer et al. 1984) and peculiar morphology in the optical (Vorontsov-Vel'yaminov 1977) (cf. Fig. 1, this paper). Further evidence for its merger interpretation has been provided by the detection of two centrally located nuclei separated in I and r images by 1''8 (Fried & Schulz 1983) and with a relative velocity of 150 km s⁻¹ (Fried & Ulrich 1985). The double nucleus of this violent merger is also clearly seen on a filtered B-band image (Fig. 1). Evidence for shocked gas in the region between either nucleus has been provided by the detection of strong H₂ 2.12 μ m emission (van

der Werf et al. 1993) which is consistent with the LINER nature diagnosed from the optical spectrum (Fosbury & Wall 1979).

The merging in NGC 6240 is accompanied by a strong nuclear starburst particularly showing up in the 2.3 μ m vibrational absorption features arising from a substantial population of red supergiants (Rieke et al. 1985, Lester et al. 1988, van der Werf et al. 1993).

The morphologically complex H α + [NII] emission pattern of NGC 6240 with loops extending out to 60 kpc and a total luminosity of 1.7×10^{42} erg s⁻¹ (Heckman et al. 1987) witnesses a starburst-driven galactic superwind. On smaller scales ($\lesssim 8$ kpc) effects of these strong gas motions, symmetrically to the nuclei, are seen in maps of the H α -equivalent width (Fig. 3, left). In this region enhanced emission from ionized gas is detected in the U-B map (Fig. 3, middle).

ROSAT PSPC maps (Fricke & Papaderos 1996) reveal a nuclear source accompanied by a very extended (2') and one-sided soft source towards the West very closely following the H α maps of Heckman et al. (1987, see above).

The soft (0.1-2.4 keV) emission of NGC 6240 can be described by a thermal bremsstrahlung model with a temperature $kT = (0.8_{-0.3}^{+0.5})$ keV and an intrinsic absorbing column density of $(1.1_{-0.7}^{+1.2}) \times 10^{21}$ cm⁻². The same model yields an intrinsic luminosity of $(3.1_{-0.9}^{+1.2}) \times 10^{42}$ erg s⁻¹.

Integration of radial intensity profiles of the PSPC-data yield a $\sim 40\%$ contribution of the extended emission to the 0.1-2.4 keV luminosity of the source. Furthermore, the extended nature of the X-ray emission in NGC 6240 is evident from the HRI-map superposed on the R-band image (Fig. 1, middle). In the right panel of the same figure the intensity distribution of the extended HRI emission reaching out to $\sim 50''$ is compared to the point response function (PRF) of the HRI and to the H α intensity distribution. The extended emission of $\sim 1.2 \times 10^{42}$ erg s⁻¹ (40% of the total soft X-ray emission) can naturally be explained by a starburst wind ISM/halo interaction. Decomposition of surface brightness profiles (cf. Fig. 2) yields an absolute B-magnitude of -21.2 mag for the starburst component of NGC 6240. With this luminosity, from the models of Leitherer & Heckman (1995), and adopting a

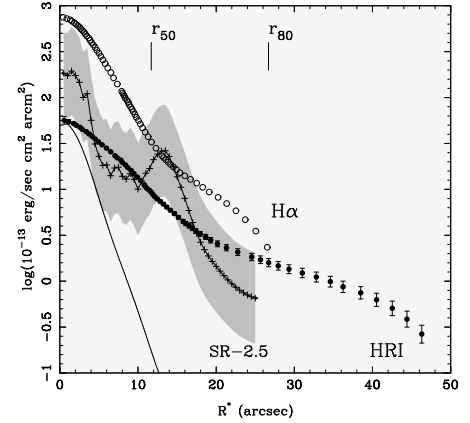


Fig. 1. left: B-band exposure of NGC 6240. Contours, corrected for galactic extinction ($A_B=0.29$ mag) are shown at the intensities from 20.5 to 26 mag arcsec $^{-2}$ in steps of 0.5 mag. Either nucleus is visible in the inset to the upper-right, displaying a filtered map of the central $12'' \times 12''$ region of the system. **middle:** ROSAT HRI exposure of NGC 6240 overlaid to a B-band exposure. The outermost contour corresponds to an intensity 7 counts ksec $^{-1}$ arcmin $^{-2}$ above the background. **right:** Radial intensity profiles of the X-ray emission derived from ROSAT HRI maps. The radii encircling 50% and 80% of the X-ray flux of the source were determined to $r_{50}=11''.7$ and $r_{80}=26''.7$, i.e. they are considerably larger than the radii $r_{50}=3''.3$ and $r_{80}=5''.9$ of the on-flight instrumental PRF (solid curve). This diagram shows that NGC 6240 is an extended X-ray source in agreement with the result by Fricke & Papaderos (1996). The shaded region displays the radial distribution of the HRI softness ratio SR (cf. Wilson et al. 1992). The H α -intensity distribution is shown by the open circles.

burst duration of ~ 25 Myr we obtain a *mechanical* energy output from the starburst of $\sim 10^{43}$ erg s $^{-1}$. The Suchkov et al. (1994) starburst wind model invoking a shocked ISM/halo then allows to account for the 40% diffuse X-ray emission inferred above. This starburst interpretation of the extended X-ray emission in NGC 6240 is not to be confused with the situation at higher energies. ASCA-observations (Iwasawa & Comastri 1998) indicate

that for an energy > 3 keV the X-ray emission of NGC 6240 is dominated by reflection of photons from a hidden AGN obscured by at least a 2×10^{24} cm $^{-2}$ column density of molecular gas. This is consistent with the evidence from the B-R map (Fig. 3, right) and the B-R profile (Fig. 2) of steadily increasing colours towards the nuclear region.

3. Correlations of Observables for a dynamical sequence

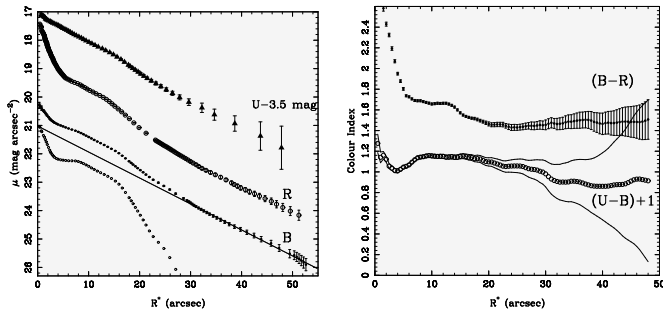


Fig. 2. (a) Surface brightness profiles of NGC 6240 in U, B and R. Note the outer exponential intensity decrease for radii $> 30''$. Profile decomposition into an exponential component (solid line) and the excess luminosity (small open circles) is shown for the B-band profile. (b) Radial B-R and U-B colour distribution. For radii $\lesssim 6''$ the B-R profile shows a gradient of 0.4 mag kpc $^{-1}$ and attains a central value $\gtrsim 2.6$ mag. This reddening is not due to superimposed H α -Emission which contribution was estimated to $\sim 6\%$ to the R-band luminosity within the central region but instead of intrinsic absorption.

Recently a first attempt has been made to discuss HRI and PSPC data for an *evolutionary sample* of 8 interacting/merging galaxies along essentially the Toomre (1977) merging sequence (Read & Ponman 1998). We discuss here a more extended sample of 22 interacting systems representing widely different dynamical stages, ranging from weak gravitational interactions through close encounters to completely merged systems. Included in this sample are the two objects NGC 2623 and AM 1146-270 from Read & Ponman (1998) and the objects Arp 284, NGC 7252 and NGC 6240, thoroughly discussed by us elsewhere (Papaderos & Fricke 1998, Fricke-v. Alvensleben et al. 1998, this paper). Besides the X-ray luminosities L_X , we determined from surface photometry of PSPC-maps the ratios of extended to pointlike emission, e/p.

A tight correspondence is found between $\log(L_X/L_B)$ and $\log(L_X)$ (Fig. 4a) and, less pronounced, for $\log(L_X/L_B)$ vs. $\log(L_{FIR}/L_B)$ (Fig. 4b). Such relations support the view that the enhanced X-ray emission in merging systems is closely linked to the strength of the induced starburst activity. The development of extended

Fig. 3. left: $H\alpha$ -equivalent width $EW(H\alpha)$ map of the central region of NGC 6240 ($D=98$ Mpc). The overlaid contours, computed from a filtered B-band image, delineate the complex morphological structure of the merging system. The $EW(H\alpha)$ shows two enhancements symmetrically to the nuclei where it attains values $\gtrsim 260 \text{ \AA}$. At the nuclear region $EW(H\alpha)$ decreases to $\lesssim 180 \text{ \AA}$. The $EW(H\alpha)$ morphology is most likely not due to the decreasing surface brightness of the stellar continuum in the vicinity of the nuclei but witnesses a kinematically perturbed warm gas component. The position of the nuclei is indicated in the inset (upper-right) by crosses. **middle:** U–B map of NGC 6240. The overlaid contours have the same meaning as in the diagram to the left. The reddest regions (> 0.3 mag) are aligned with the major axis of the system between 4 and 8 kpc from the nuclear region. The regions indicated by the circles display blue U–B colours ranging between -0.3 mag (region b) and -0.6 mag (region a). Such colours, being much bluer than the average U–B index of $\sim +0.1$ mag for radii $> 10''$ (cf. Fig. 2), point to the presence of strong emission by ionized gas, especially $[OII]\lambda\lambda 3726, 3729$, in the vicinity of the nuclear region of NGC 6240, in agreement with the $EW(H\alpha)$ -morphology (cf. Barbieri et al. 1993). **right:** The diffuse B–R colour distribution does not show any correspondence to the optical morphology (contour lines) and attains values $\gtrsim 2.6$ mag towards the nuclear region (cf. Fig. 2). This indicates the increasing extinction within NGC 6240.

emission, with the e/p -ratio being typically > 0.5 , seems to be a common feature of all mergers. No evidence for a relation between e/p and $\log(L_{FIR}/L_B)$ is observed (Fig. 4c). We arranged our 22 objects tentatively along a qualitative merger sequence mainly being guided by the interaction strength and morphology of the systems (distances, disturbances, tails, bridges, brightness profiles). In Fig. 4d we plot $\log(L_X/L_B)$ and $\log(L_{FIR}/L_B)$ along this sequence.

Three phases can be roughly distinguished. On the l.h.s are located the early, detached systems like Arp 284 which experience a first interaction-induced starburst while the r.h.s is populated by the advanced mergers with strong nuclear starbursts, like NGC 6240. The intermediate portion represents those systems which are just starting the merging process like the Antennae (NGC 4038/39). The strong decline in the FIR- and X-ray luminosity on the right end represents the post merger stage and the transition of the merger into an elliptical galaxy as seen in NGC 7252.

Observations of systems populating the intermediate phase show an increasing pile-up of obscuring material

(mainly molecular gas) enshrouding the starburst region. In this phase the FIR luminosity starts to rise until dominating the bolometric luminosity for objects beyond NGC 6240 on the sequence.

4. Discussion and conclusions

The evolution of individual systems along this sequence may strongly depend on the intrinsic properties of the colliding galaxies as has been shown in dissipative numerical simulations by Mihos & Hernquist (1996; cf. their Fig. 10): The disk/halo systems suffer their main burst early in the encounter and hardly burst again, while the disk/bulge/halo systems manage to retain their gas almost until complete merging, in order then to suffer a strong, short-lived burst much later than the bulgeless systems. For the merged systems it is difficult to verify a posteriori whether the original interaction partners were bulge systems or not. These important parameters are not directly known. Dissipative numerical simulations with very high particle numbers may help here. Furthermore, it is not well understood, how the formation of non-thermal activity (AGNs) fits into the merger sequence. The sample

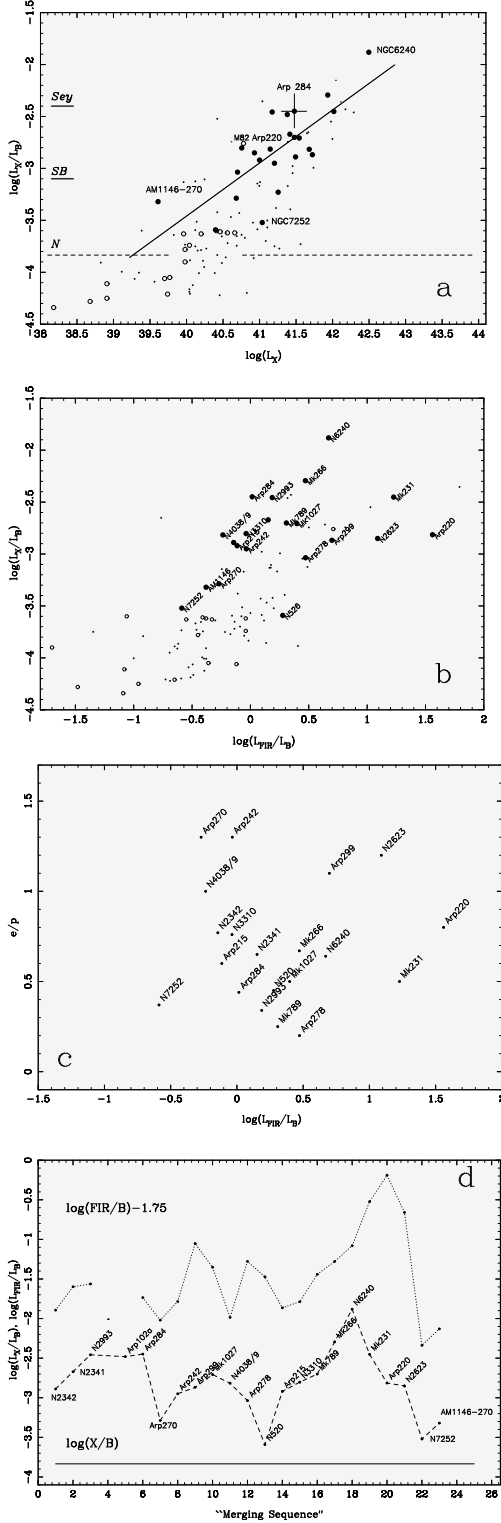


Fig. 4. a: Comparison of the X-ray luminosity $\log(L_X)$ with the $\log(L_X/L_B)$ -ratio for colliding starburst galaxies. We include NGC 2623 and AM 1146-270 (Read & Ponman 1998), Arp 284 (Papaderos & Fricke 1998) and NGC 7252 (Fritze v.-Alvensleben et al. 1998). The samples of David et al. (1992) and Read et al. (1997) are shown by dots and open circles, respectively. **b:** $\log(L_{FIR}/L_B)$ vs. $\log(L_X/L_B)$ -diagram. **c:** $\log(L_{FIR}/L_B)$ - vs. e/p -ratio. **d:** Evolution of the $\log(L_X/L_B)$ and $\log(L_{FIR}/L_B)$ ratios along a tentative merging sequence.

investigated here shows the occurrence of AGNs in all major phases of the sequence. Also here very high-resolution gas/star numerical simulations are required to investigate the inflow conditions at the centers of interacting/merging systems.

The extended X-ray contribution e/p does not show any conspicuous evolution along the merger sequence. This extended component is in all phases related to the starburst activity and the shock-heating of the ambient gas by starburst winds. This mechanism is certainly not responsible for the extended X-ray emission observed in the halos of elliptical galaxies (Fabbiano 1989). In fact, in the young merger remnant NGC 7252 an extended X-ray halo is not yet present.

Around such systems, however, ample mechanical energy is stored in the gravitationally bound tidal material. During the ensuing passive evolution this material will fall back onto the main body of the remnant and will thereby form an extended X-ray halo as seen in Ellipticals within a couple of Gyrs. Model calculations for this process will be important (cf. Hibbard & Mihos 1995).

The example of Arp 284 (Papaderos & Fricke 1998) may indicate that off-nuclear X-ray sources may form quite early during interactions in the shocked H I-gas. Such sources will later-on be smeared out and may contribute to halo formation at a stage prior to completed merging. More examples of this type should be found.

Understanding of the merger sequence, e.g. the evolution of global parameters like the luminosities in different energy bands and the morphology of extended emission in successive stages of merging is still in a rudimentary state. The complexity, in particular regarding the generation of X-rays, is enormous as seen from the detailed results for individual objects (cf. Papaderos & Fricke 1998, Fritze, Read & Ponman 1998). However, first patterns seem to emerge.

Acknowledgements. We thank W. Pietsch and K. Bischoff for observing an U-band frame of NGC 6240. P. Papaderos thanks K. Bischoff for assistance during observations at Calar Alto. This work was supported by the Deutsche Agentur für Raumfahrtangelegenheiten (DARA) grant 50 OR 9407 6.

References

- Barbieri, C. et al. 1993, A&A 273, L1
- David, L.P., et al. 1992, ApJ 388, 82
- Fabbiano, G. 1989, ARA&A 27, 87
- Fosbury, R.A.E., Wall, J.V. 1979, MNRAS 189, 79
- Fricke, K.J., Papaderos, P. 1996, in *Röntgenstrahlung from the Universe*, eds. H.U. Zimmermann, Trümper, J.E., Yorke, H., p. 377
- Fried, J.W., Schulz, H. 1983, A&A 118, 166
- Fried, J.W., Ulrich, H. 1985, A&A 152, L14
- Fritze v.-Alvensleben, U. et al. 1998, in prep.
- Heckman, T.M. et al. 1987, AJ 93, 276
- Hibbard, J.E., Mihos, J.C. 1995, AJ 110, 140
- Iwasawa, K., Comastri, A. 1998, MNRAS 297, 1219
- Leitherer, C., Heckman, T.M. 1995, ApJS 96, 9
- Lester, D.F. et al. 1988, ApJ 329, 641

- Mihos, J.C. & Hernquist, L. 1996, ApJ 464, 641
Papaderos, P., Fricke, K.J. 1998, A&A 338, 31
Read, A.M. et al. 1997, MNRAS, 286, 626
Read, A.M., Ponman, T.J. 1998, MNRAS 297, 143
Rieke, G.H. et al. 1985, ApJ 290, 116
Soifer, B.T. et al. 1984, ApJ 278, L71
Suchkov, A.A., et al. 1994, ApJ 430, 511
Toomre, A. 1977, in *Evolution of Galaxies and Stellar Populations*, p. 401
Wilson, A.S. et al. 1992, ApJ 391, L75
Vorontsov-Vel'yaminov, B.A. 1977, A&AS 28, 1
van der Werf, P.P. et al. 1993, ApJ 405, 522

This figure "ngc6240f1.gif" is available in "gif" format from:

<http://arxiv.org/ps/astro-ph/9810144v1>

This figure "ngc6240f2.gif" is available in "gif" format from:

<http://arxiv.org/ps/astro-ph/9810144v1>

This figure "ngc6240f6.gif" is available in "gif" format from:

<http://arxiv.org/ps/astro-ph/9810144v1>

This figure "ngc6240f7.gif" is available in "gif" format from:

<http://arxiv.org/ps/astro-ph/9810144v1>

This figure "ngc6240f8.gif" is available in "gif" format from:

<http://arxiv.org/ps/astro-ph/9810144v1>